PHYSICAL REVIEW A

GENERAL PHYSICS

THIRD SERIES, VOLUME 35, NUMBER 7 APRIL 1, 1987

Fine structure of the Rydberg levels in helium derived from experiment and theory

Edward S. Chang

Department of Physics and Astronomy, University of Massachusetts, Amherst, Massachusetts 01003

(Received 4 August 1986)

The fine-structure levels of helium from microwave data are coalesced into a single-term-value table by means of theories. It is found to yield transition frequencies in excellent agreement with some diode laser measurements and a consistent ionization energy of 198 310.772 2(5) cm^{-1}. This value is 1 order of magnitude higher in precision and in accord with Martin's value [Phys. Rev. A **29**, 1883 (1984)], subject to the same assumption on the $2\,^1P$ level. A semiempirical theory is developed and fitted to all levels ($L \geq 2$). The result suggests a modification in the usual usage of the polarization formula for the direct energy and extends its utility to the exchange energy.

I. INTRODUCTION

The description of a multielectron system greatly simplifies when one optical electron is excited and moves in the field of an ionic core in the S state. Such excited states are called quasihydrogenic or nonpenetrating Rydberg states if the orbital angular momentum L is sufficient to preclude the electron's motion from the core region. Based on this simple picture, the polarization formula has proven to be a very useful tool in analyzing atomic spectra.[1,2] When the core and the optical electron have spin angular momenta, additional magnetic interactions will intermix with the electrostatic exchange interaction to produce fine structure.

A particularly simple example is the two-electron system. Here the one-electron core is hydrogenic, so all its properties pertaining to long-range interactions can be calculated analytically as in the works of Drachman.[3,4] In fact, his calculations enable one to determine helium term values to an accuracy of 3×10^{-5} cm^{-1} for G ($L=4$) and 3×10^{-7} cm^{-1} for H ($L=5$) states, provided that the electrostatic direct spin-free energy can be successfully disentangled from the fine structure. A complete theory for the helium fine structure has been formulated by Cok and Lundeen.[5] They have tabulated results of elaborate computations of three radial integrals in the magnetic fine structure for each separate value of L and the principal quantum number n. For the electrostatic exchange energy, accurate variational calculations have been performed[6] for D states.

An abundance of high-precision experimental data from microwave and field-crossing measurements in helium (including some computed energy levels) has been collected by Farley *et al.*[7] They analyzed these one- and two-photon transitions between fine-structure levels within the same n manifold according to the Rayleigh-Ritz principle, and obtained a single set of self-consistent global-fit data for each value of n. From the viewpoint of traditional spectroscopy, Martin[8] has compiled helium experimental energies believed to be accurate to 0.01 cm^{-1}. Later he reevaluated the data in light of new laser measurements for low-n and -L substates.[9] The precision of many energies has improved beyond 0.001 cm^{-1}. By combining these energies with theoretical term values, he was able to determine the ionization energy within an error of 0.004 cm^{-1} with 95% confidence.[9]

In the present work the best experimental data and theory are collected to produce a unique energy scheme of high precision and self-consistency for helium. For the range of $5\leq n\leq 12$ and $L\geq 2$, the term values are accurate to the 10^{-5} cm^{-1} level. By an independent test using the diode laser measurement of the $5D$-$6F$ transitions,[10] the crucial inter-n interval is found to be superior to other works.[6,8,9,11,12] Similarly the ionization energy derived from these term values is more precise than and consistent with the recent values.[6,9]

The present energy scheme is based on the global-fit data[7] enriched with the higher-L measurements[13] for $n=7$ and 8. A simplified fine-structure theory is developed in Sec. II, where the sublevels are described in terms of the following three parameters for each value of n and L. The magnetic constant h depends theoretically on n and L in a trivial way, and in Sec. III theoretical values are compared with those derived from the experimental data. The exchange energy X can be extracted from the global-fit data in two ways. The discrepancy among the two values is a test of the theory as well as of the data's quality. For the D states, precise variational

calculations[6] of X are available for comparison. These tests show that for the present purposes the simplified theory may be used instead of the more elaborate theory of Cok and Lundeen.[5] Finally the direct energy may be taken from Drachman's Theory[3] for the highest-L complex for which experimental measurements are available. Then global-fit energies for each n can be fixed to a common energy scale, most conveniently expressed as term values in Sec. IV.

In Sec. V the status of the polarization formula is elucidated by utilizing the present data in Edlén plots.[1] As already predicted by other theories,[3,14] the result is *not* a single straight line. However, the direct energy shifts for each value of L *do* form a straight line as well as the quantity n^3X. These features may be combined into a semiempirical theory where *linear* extrapolations in n (unlike the nonlinear ones in the global-fit data[7]) may be made to fill in missing or low-precision data. Thus improvement is made on the global-fit data in the regime of low n, where the original measurements are sparse and less accurate.

To facilitate comparison with one-photon measurements, general multiplet intensities are given in Sec. VI, accounting for singlet-triplet mixing. For the $5D$-$6F$ transition, specific multiplet intensities are evaluated. An approximate procedure is described for comparison with the diode laser measurement,[10] where the fine structure has not been completely resolved. In Sec. VII, the ionization energy is determined from the present term values. Finally, in Sec. VIII I discuss the implications of the semiempirical theory for other atoms.

II. SIMPLIFIED FINE-STRUCTURE THEORY

The present system consists of a nucleus of charge Z and negligible spin, a spherical ionic core ($L_c=0$) with spin S_c, and an optical electron with orbital angular momentum $L\geq 2$ (and, of course, spin $s=\frac{1}{2}$). It is convenient to separate the Hamiltonian of the system into a magnetic term $H_{\rm mag}$ which explicitly depends on spin and an electrostatic term $H_{\rm es}$ which includes exchange and all relativistic effects that are independent of spin.

The magnetic-fine-structure theory has been accurately given by Cok and Lundeen.[5] By applying the Heisenberg[15] (nonpenetrating) approximation to the optical electron, the spin-dependent Hamiltonian greatly simplifies to

$$\begin{aligned}H_{\rm mag}=(a_0\alpha^2)/(mr^3)[&\tfrac{1}{4}(Z-3)\boldsymbol{l}\cdot(\mathbf{s}+\mathbf{S}_c)\\&+\tfrac{1}{4}(Z+1)\boldsymbol{l}\cdot(\mathbf{s}-\mathbf{S}_c)\\&+\mathbf{s}\cdot\mathbf{S}_c-3(\mathbf{s}\cdot\hat{\mathbf{r}})(\mathbf{S}_c\cdot\hat{\mathbf{r}})]\ .\end{aligned}\tag{1}$$

In Eq. (1), m is the reduced mass of the electron, α the fine-structure constant, and r the electron's distance in Bohr radii (a_0) from the nucleus. Since the atomic core is assumed to be in an S state, the total orbital angular momentum L is identical to l. The magnetic Hamiltonian may be broken up into a spin-orbit, a spin—other-orbit, and a spin-spin term. Thus

$$H_{\rm mag}=H_{ls}+H_{lS_c}+H_{sS_c}\ ,\tag{2}$$

where

$$H_{ls}=(Z-1)(2\boldsymbol{l}\cdot\mathbf{s})h\ ,\tag{3}$$

$$H_{lS_c}=-2(2\boldsymbol{l}\cdot\mathbf{S}_c)h\ ,\tag{4}$$

and

$$H_{sS_c}=4[\mathbf{s}\cdot\mathbf{S}_c-3(\mathbf{s}\cdot\hat{\mathbf{r}})(\mathbf{S}_c\cdot\hat{\mathbf{r}})]h\ .\tag{5}$$

These expressions agree with those in Palfrey and Lundeen.[16] In the Heisenberg approximation, the magnetic parameter is

$$h=\tfrac{1}{2}\alpha^2R\langle r^{-3}\rangle_{nL}=\alpha^2R[n^3(2L+1)L(L+1)]^{-1}\ .\tag{6}$$

The matrix elements in Eqs. (3) and (4) are trivially evaluated in their appropriate l-s representations. Following Bethe and Salpeter,[17] the operator in Eq. (5) is found to be diagonal in the L-S representations, with matrix element given by

$$(LSJ\mid H_{sS_c}\mid LSJ)=-4Yh/(2L-1)(2L+3)\ ,\tag{7}$$

where

$$\begin{aligned}Y=&L(L+1)[S(S+1)-S_c(S_c+1)+\tfrac{3}{4}]\\&-\tfrac{3}{4}\{[J(J+1)-L(L+1)-S(S+1)]\\&\quad+[J(J+1)-L(L+1)-S(S+1)]^2\}\ .\end{aligned}\tag{8}$$

Using Racah algebra,[18] the matrix elements of Eqs. (3) and (4) are easily transformed to the same L-S representation as follows,

$$\begin{aligned}&(L(sS_c)SJ\mid H_{ls}\mid L(sS_c)S'J)\\&=2(Z-1)hL(L+1)[(2S+1)(2S'+1)]^{1/2}\\&\times\left[\begin{Bmatrix}L&\frac{1}{2}&L+\frac{1}{2}\\S_c&J&S\end{Bmatrix}\begin{Bmatrix}L&\frac{1}{2}&L+\frac{1}{2}\\S_c&J&S'\end{Bmatrix}\right.\\&\left.-\begin{Bmatrix}L&\frac{1}{2}&L-\frac{1}{2}\\S_c&J&S\end{Bmatrix}\begin{Bmatrix}L&\frac{1}{2}&L-\frac{1}{2}\\S_c&J&S'\end{Bmatrix}\right]\ ,\end{aligned}\tag{9}$$

and

TABLE I. Matrix elements of $H_{\rm mag}$ in terms of h [Eq. (6)] for $S_c=\frac{1}{2}$.

S	S'	J	H_{ls}	H_{lS_c}	H_{sS_c}
0	0	L	0	0	0
0	1	L	$(Z-1)\sqrt{L(L+1)}$	$2\sqrt{L(L+1)}$	0
1	1	$L-1$	$-(Z-1)(L+1)$	$2L+2$	$(2L+2)/(2L-1)$
1	1	L	$-(Z-1)$	2	-2
1	1	$L+1$	$(Z-1)L$	$-2L$	$2L/(2L+3)$

$$
\begin{aligned}
&((L(sS_c)SJ \mid H_{lS_c} \mid L(sS_c)S'J)) \\
&\quad=(-1)^{S'-S+1}4h[(2S+1)(2S'+1)]^{1/2} \\
&\quad\times\left[(J+1)[(J+\tfrac{1}{2})(J+\tfrac{3}{2})-L(L+1)-S_c(S_c+1)]\begin{Bmatrix} L & S_c & J+\frac{1}{2} \\ \frac{1}{2} & J & S \end{Bmatrix}\begin{Bmatrix} L & S_c & J+\frac{1}{2} \\ \frac{1}{2} & J & S' \end{Bmatrix}\right. \\
&\qquad\left.+J[(J-\tfrac{1}{2})(J+\tfrac{1}{2})-L(L+1)-S_c(S_c+1)]\begin{Bmatrix} L & S_c & J-\frac{1}{2} \\ \frac{1}{2} & J & S \end{Bmatrix}\begin{Bmatrix} L & S_c & J-\frac{1}{2} \\ \frac{1}{2} & J & S' \end{Bmatrix}\right] . \qquad (10)
\end{aligned}
$$

In Eqs. (9) and (10),

$$\begin{Bmatrix} j_1 & j_2 & j_3 \\ j_4 & j_5 & j_6 \end{Bmatrix}$$

is the usual 6-j symbol.

For the heliumlike configuration $1s\,nl$, the allowed quantum numbers are $S_c=\frac{1}{2}$, $S=0,1$, and $J=L-1$, L,$L+1$. Table I lists the matrix elements of Eqs. (3), (4), and (5) with these values of L, S, and J. The electrostatic energy can be written in general[19] as the sum of a direct term D and an exchange term X,

$$
\begin{aligned}
E_{\rm es}&=D+[-\tfrac{1}{2}+S_c(S_c+1)+\tfrac{3}{4}-S(S+1)]X \\
&=D\pm(S_c+\tfrac{1}{2})X,\quad S=S_c\mp\tfrac{1}{2} . \qquad (11)
\end{aligned}
$$

Combining with the spin-dependent Hamiltonian, the fine structure energies are obtained by diagonalizing the total Hamiltonian in the L-S representation,

$$
\begin{aligned}
E(L\,1\,L-1)&=D-X+[3-Z+2(2L-1)^{-1}](L+1)h , \\
E(L\,1\,L+1)&=D-X+[-3+Z+2(2L+3)^{-1}]Lh , \\
E(L\,0\,L)&=D-(Z-1)h/2+\{[X+(Z-1)h/2]^2 \\
&\qquad+(Z+1)^2L(L+1)h^2\}^{1/2} , \\
E(L\,1\,L)&=D-(Z-1)h/2-\{[X+(Z-1)h/2]^2 \\
&\qquad+(Z+1)^2L(L+1)h^2\}^{1/2} . \qquad (12)
\end{aligned}
$$

For helium ($Z=2$), accurate experimental energies are available[7] up to $n=12$. Then Eq. (12) may be inverted as a test of the simplified theory. In particular, the three unknowns D, X, and h can be evaluated from each set of four fine-structure levels, with an extra condition to check for consistency. One finds

$$
\begin{aligned}
h&=[E(L\,1\,L-1)-E(L\,1\,L+1)] \\
&\quad\times[1-6/(4L^2+4L+3)]/(2L+1) , \qquad (13) \\
D&=\tfrac{1}{2}[E(L\,0\,L)+E(L\,1\,L)] \\
&\quad+\tfrac{1}{2}[E(L\,1\,L-1)-E(L\,1\,L+1)] \\
&\quad\times[1-6/(4L^2+4L+3)]/(2L+1) , \qquad (14) \\
X&=\tfrac{1}{2}[E(L\,0\,L)+E(L\,1\,L) \\
&\quad-E(L\,1\,L-1)-E(L\,1\,L+1)] \\
&\quad+8L(L+1)[E(L\,1\,L-1)-E(L\,1\,L+1)] \\
&\quad\times[(2L+1)(4L^2+4L+3)]^{-1} , \qquad (15)
\end{aligned}
$$

and

$$(X+h/2)^2+9L(L+1)h^2=[E(L\,0\,L)-E(L\,1\,L)]^2/4 . \qquad (16)$$

Of special importance is Eq. (14) which allows one to correctly extract the spinless electrostatic direct energy from the four fine-structure sublevels. As discussed by Curtis and Ramanujam[14] (CR), several other procedures have been adopted for this quantity in application of the polarization theory. For their study, only the first square bracket was used. On the other hand, Edlén[1] assumed a spinless core, and obtained an expression similar to Eq. (14) except that the last square bracket was replaced by unity. Yet others utilized the statistical mean, which removes the magnetic interaction (in contradiction to CR), but leaves a residual exchange term of $-X/2$.

In conventional spectroscopy, the triplet sublevels are usually unresolved. The barycenter position, ${}^3L_{\rm av}$, weighting each sublevel by $(2J+1)$, is not free from magnetic

interactions in the second order. For low L states, the barycenter is found from Eq. (12) to be

$$^3L_{\rm av} \simeq -X - 3L(L+1)h^2/2X \ ,$$

where $h \ll X$. For example, the $3D$ residual magnetic interaction represented by the last term is 0.02 cm^{-1}, and falls off as n^{-3} for larger n. These variations in the treatment of both experimental data and computational results make detailed comparisons of other works with the present work difficult.

III. VERIFICATION WITH THE GLOBAL-FIT DATA AND DRACHMAN'S THEORY

For the present purpose, a convenient data base is the "global-fit" compilation of Farley *et al.*[7] They have collected mostly experimental and some theoretical data for all transitions within the same n manifold for n ranging from 3 to 12. Each datum was weighted statistically. Then fine-structure energy levels were obtained subject to the Rayleigh-Ritz combination principle. Their precisions were usually of the order 10^{-5} cm^{-1} for $n=7$ or higher. However, they worsened rapidly with decreasing n as more reliance was placed in theory and in extrapolation of data. For $n=7$ and 8, even more precise data involving the H ($L=5$) states are available from the work of Cok and Lundeen.[13]

From the above set of data, the three parameters in Eqs. (13)—(15) are evaluated for each value of n and L. In Table II the actual fine-structure splittings, $^3L_{L-1}$-$^3L_{L+1}$, are given rather than h. From Eq. (13), h is related to the tabulated quantities simply by the multiplicative factor 0.155 56, 0.126 05, and 0.103 08 for $L=2$, 3, and 4, respectively. It is seen that the simple theoretical values given by Eq. (6) lie within experimental error for $L=3,4$. However, for the slightly penetrating D levels, theoretical values appear to fall below the experimental ones by 1%. Even the elaborate theory of Cok and Lundeen[5] improved the agreement by only a factor of 2. In contrast, a discrepancy of 20% occurs for the penetrating P levels.

The direct energies D can only be evaluated relative to another L level with the same value of n. These so-called electrostatic intervals agree with those of Cok and Lundeen[13] within 10^{-5} cm^{-1}. Their ramifications for polarization theory will be discussed later in Sec. V. Table III shows the exchange energies X as determined by Eq. (15) and by Eq. (16) using Eq. (13) to eliminate h. Usually the two values agree very well, reflecting the consistency of the simplified theory with experiment and the quality of the data. For comparison, values from Cok and Lundeen's extended adiabatic approach[5] are also shown in both Tables II and III. For the fine-structure splitting, no appreciable difference is seen except in the lowest few nD states. Here their elaborate calculations lead to somewhat better results. Similarly their exchange energies agree with the present ones within their stated errors. Further comparison for nD states ($n \leq 8$) can be made with the high-precision variational results from Kono and Hattori.[6] They all concur very well except possibly for the $3D$ value of Cok and Lundeen. In the simplistic Heisenberg approximation,[15] $X(n,2)$ is too low by a factor of 3 and $X(n,3)$ by a factor of 2. $X(n,4)$ is less than 10^{-6} cm^{-1} and therefore cannot be determined from the data with the present precision.

For $n \leq 6$, the larger discrepancy between the exchange energies from Eqs. (15) and (16) is due to the poorer quality in the global-fit data. As high-precision measurements become unavailable, more and more reliance is placed on extrapolation from higher-n data. It is known that X must asymptotically approach n^{-3}, but at low values deviation is considerable. In fact, for the $4F$ level, the X value from Eq. (15) has an uncertainty equal to the value itself, and from Eq. (16), the X value becomes complex, indicating an underestimation of the $^3F_3$-$^1F_3$ splitting. In order to place the energy levels on an absolute scale, it is necessary to examine the direct energy more closely. It turns out that both D and X, using appropriate scaling, can be plotted on straight-line graphs. Thus, accurate extrapolation may be made as discussed in Sec. V.

TABLE II. Fine-structure splitting $^3L_{L-1}$-$^3L_{L+1}$. (Values in 10^{-5} cm^{-1}.) Experimental values are from Ref. 3. Theoretical values are from Eq. (13).

n \ L	2			3		4	
	Expt.	Theor.	CL[a]	Expt.	Theor.	Expt.	Theor.
3	4672(3)	4637	4654				
4	1972(1)	1956	1966	890(240)	862		
5	1010(1)	1002	1007	449(50)	442	261(49)	252
6	585(1)	580	582	258(5)	256	149(8)	146
7	369(1)	365	366	160(1)	161	93(1)	92
8	247(0)	245		108(1)	108	62(1)	62
9	173(2)	172	172	76(2)	76	43(2)	43
10	126(2)	125	125	56(2)	55	31(2)	32
11	95(1)	94		42(1)	42	23(1)	24
12	73(1)	73		32(1)	32	18(1)	18

[a]Cok and Lundeen theory, Ref. 13. Values for $L=3$ and 4 are identical to theory.

TABLE III. Exchange energy X in 10^{-5} cm^{-1}.

n	Eq. (15)	Eq. (16)	CL[a]	KH[b]	Improved[c]
			$L=2$		
3	170 469(5)[d]	170 442[d]	169 617(333)	170 580(30)	170 456(13)
4	98 510(10)[d]	98 500	98 431(132)	98 520(20)	98 505(5)
5	56 749(25)	56 805	56 829(77)	56 820(10)	56 810(5)
6	34 890(6)	34 883	34 884(50)	34 890(10)	34 877(3)
7	22 738(1)	22 734	22 736(1)	22 740	
8	15 566(1)	15 563	15 564(60)	15 570	
9	11 092(2)	11 090	11 091(1)		
10	8170(2)	8168	8142(50)		
11	6184(1)	6183	6158(50)		
12	4790(1)	4790			
			$L=3$		
4	294(240)	e			130(3)
5	240(50)	173			201(1)
6	166(9)	152	159		158(1)
7	112(1)	115	113		
8	82(1)	81	82		
9	59(2)	59	60		
10	46(2)	44	46		
11	34(1)	34	35		
12	27(1)	28	27		

[a]Cok and Lundeen, Ref. 5.
[b]Kono and Hattori, Ref. 6.
[c]Derived from Table V.
[d]Derived from Martin, Ref. 9, otherwise from Table IV.
[e]Value is complex. See text.

IV. DRACHMAN'S THEORY AND THE EXPERIMENTAL TERM VALUES

The direct energy D, from Eq. (14), may be regarded as a term value related to the ionization energy E_I by $t=E_I-D$. It is convenient to separate out the Rydberg term

$$t_{nL}=R(Z-1)^2/n^2+\Delta_{nL} . \tag{17}$$

Usually the Rydberg constant R_0 for He is taken[9] to be $\mu R_\infty=109\,722.273\,09(11)$ cm^{-1}, where $\mu=mM/(m+M)$ with electron m and nuclear mass M. Recently, using Jacobi coordinates, Drachman has derived a second-order nuclear recoil term,[20] which modifies the kinetic energy of the Rydberg electron by the factor $(1-m^2/M^2)$. Thus, the new appropriate Rydberg constant R is

$$R_\infty\mu(1-m^2/M^2)^{-1}=R_\infty m(M+m)/(M+2m) .$$

An obvious interpretation is that the Rydberg electron's reduced mass is relative to the entire core of mass $(M+m)$. Hence, the new Rydberg constant for He is larger than R_0 by $R_\infty m^2/M^2=0.002\,06$ cm^{-1}. So the appropriate value of R for ^{4}He is 109 722.275 15(11) from above based on an unpublished[9] R_0 or 109 722.275 20(13) cm^{-1} based on[21] $R_\infty=109\,737.315\,34(13)$ cm^{-1}.

The spin-free energy shift may be expressed as the sum of the relativistic and nonrelativistic contributions of the optical electron,

$$\Delta_{nL}=\Delta_{nL}^{(r)}+\Delta_{nL}^{(\mathrm{nr})} . \tag{18}$$

Formally the relativistic part includes the Lamb shift[9] and the "retardation correction" effect.[22] The former vanishes for states of $L\geq 2$ because it involves the Dirac δ function. The latter is usually very small, and is more conveniently treated as part of $\Delta^{(nr)}$. Therefore, the relativistic shift to the accuracy required here is simply due to increase in electron mass,[3,4]

$$\Delta_{nL}^{(r)}=\alpha^2R(Z-1)^4[n/(L+\tfrac{1}{2})-\tfrac{3}{4}]/n^4 . \tag{19}$$

Following Drachman,[3] the nonrelativistic term is separated into a first- and a second-order correction, $\Delta^{(\mathrm{nr})}=\Delta^{(1)}+\Delta^{(2)}$. The first-order term $\Delta^{(1)}$ is the sum of expectation values of inverse powers of the optical electron's distance from the nucleus r. The leading term in $\Delta^{(1)}$ is due primarily to the induced dipole polarizability of the core α_1,

$$V_4=\alpha_1\langle r^{-4}\rangle_{nL}[1+\mu_m-\tfrac{28}{27}(Z\alpha)^2-\alpha^4/4\alpha_1] . \tag{20}$$

The correction terms in the square bracket are due to mass polarization,[3] to relativistic effects on the polarizability,[4] and to the retarded potential[22] which amount to 2.74×10^{-4}, 2.21×10^{-4}, and 0.47×10^{-4}, respectively. Therefore, the net correction is only 7×10^{-6}, negligibly small except for D states where its value is 10^{-4} cm^{-1} for the lowest few n.

The second term in $\Delta^{(1)}$ is given by[3]

TABLE IV. Term values of helium.

Term	J	T_{LSJ} (cm^{-1}) $n=5$	$n=6$	Term	J	T_{LSJ} (cm^{-1}) $n=9$	$n=10$[c]
^1G	4	4389.047 01(3)[a]	3047.941 82(4)[a]	^1G	4	1354.629 91(2)[a]	1097.247 93(2)[a]
^3G	3	4389.048 70(48)	3047.942 80(8)	^3G	3	1354.630 20(2)	1097.248 15(2)
	4	4389.053 94(17)	3047.945 85(5)		4	1354.631 11(2)	1097.248 81(2)
	5	4389.051 31(49)	3047.944 29(8)		5	1354.630 63(2)	1097.248 46(2)
^1F	3	4389.538 21(11)[b]	3048.237 16(4)	^1F	3	1354.721 60(2)	1097.315 23(2)
^3F	2	4389.543 38(48)[b]	3048.240 61(9)	^3F	2	1354.722 79(2)	1097.316 13(2)
	3	4389.550 66(11)[b]	3048.244 71(4)		3	1354.723 96(2)	1097.316 98(2)
	4	4389.547 87(49)[b]	3048.243 19(9)		4	1354.723 55(2)	1097.316 69(2)
^1D	2	4392.379 04(9)[b]	3049.898 42(4)	^1D	2	1355.220 23(2)	1097.679 44(2)
^3D	1	4393.506 88(34)[b]	3050.591 66(6)[b]	^3D	1	1355.440 72(2)	1097.841 85(2)
	2	4393.516 33(34)[b]	3050.597 12(6)[b]		2	1355.442 33(2)	1097.843 02(2)
	3	4393.516 98(33)[b]	3050.597 51(6)[b]		3	1355.442 45(2)	1097.843 11(2)

Term	J	T_{LSJ} (cm^{-1}) $n=7$	$n=8$	Term	J	T_{LSJ} (cm^{-1}) $n=11$	$n=12$
^1H	5	2239.252 75(0)[a]	1714.426 76(0)[a]	^1G	4	906.814 83(1)[a]	761.975 17(1)[a]
^3H	4	2239.253 19(1)	1714.427 06(0)[a]	^3G	3	906.814 99(1)	761.975 30(1)
	5	2239.254 44(1)	1714.427 90(0)[a]		4	906.815 49(1)	761.975 64(1)
	6	2239.253 79(0)	1714.427 46(0)[a]		5	906.815 22(1)	761.975 48(1)
^1G	4	2239.297 69(1)	1714.457 58(1)	^1F	3	906.865 65(1)	762.014 46(1)[b]
^3G	3	2239.298 30(1)	1714.457 99(1)	^3F	2	906.866 33(1)	762.015 00(1)[b]
	4	2239.300 23(1)	1714.459 28(1)		3	906.866 97(1)	762.015 49(1)[b]
	5	2239.299 23(1)	1714.458 61(1)		4	906.866 75(1)	762.015 32(1)[b]
^1F	3	2239.487 90(1)	1714.586 85(1)	^1D	2	907.139 68(1)	762.225 77(1)[b]
^3F	2	2239.490 23(1)	1714.588 50(1)	^3D	1	907.262 62(1)	762.321 69(1)[b]
	3	2239.492 78(1)	1714.590 18(1)		3	907.263 57(1)	762.321 74(1)[b]
	4	2239.491 83(0)	1714.589 58(1)				
^1D	2	2240.540 58(1)	1715.294 88(1)				
^3D	1	2240.992 47(1)	1715.604 27(1)				
	2	2240.995 91(1)	1715.606 57(1)				
	3	2240.996 16(1)	1715.606 74(1)				

[a]Determined by theory.
[b]Not based on experiments. Uncertainty may be substantially larger than the quoted one.
[c]More accurate values may be obtained from Ref. 16.

$$V_6=(\alpha_2-6\beta_1)\langle r^{-6}\rangle_{nL} , \tag{21}$$

where α_2 is the quadrupole polarizability and β_1 the nonadiabatic correction to the dipole polarization. Finally, the last term (V_7+V_8) contains all other higher-order corrections. It turns out that the last term is numerically larger than V_6 for F states ($L=3$), but smaller by at least an order of magnitude for higher values of L. Regarding $\Delta^{(1)}$ as an asymptotic series, Drachman has determined first-order shifts to be as follows[3] (small errors corrected later[4] are negligible small for the present purpose),

$$\Delta^{(1)}=\begin{cases} V_4+V_6/2\pm V_6/2 , & \text{(22a)} \\ V_4+V_6+(V_7+V_8)/2\pm(V_7+V_8)/2 . & \text{(22b)} \end{cases}$$

For $L\geq 4$, the uncertainty is no more than 3×10^{-5} cm^{-1} or 1 MHz (1 MHz$=3.335\,64\times10^{-5}$ cm^{-1}).

The second-order polarization shifts $\Delta^{(2)}$ have also been tabulated by Drachman[4] for $L\geq 3$. They are much smaller than either the exchange or the fine-structure terms, and are less than 3×10^{-5} cm^{-1} for G and higher-L levels.

The above theory provides a framework for fixing high-L Rydberg levels to an absolute energy scale. For $n=5$–12, G levels are always available in the global-fit data of Farley *et al.*[7] Further, in the cases of $n=7$ and 8, H levels from Lundeen's work[13] can provide even more accurate absolute term values. If the microwave (intra-n) data were sufficiently accurate, the uncertainty in the absolute energies would be about 1 and 0.01 MHz for G and H levels, respectively. It is recalled that for G levels, X is less than 10^{-6} cm^{-1} (and decreases by about 2 orders of magnitude for each successively higher value of L). Therefore it may safely be neglected in fixing the singlet sublevel from Eq. (12) to the absolute scale for each n. From then on, the above one- and two-photon microwave data are utilized to construct the experimental energy-level scheme in Table IV. Details of actual transitions employed are relegated to the Appendix. It should be noted that the energy levels thus found are accurate to 1 or 2 times 10^{-5} cm^{-1}. However, the situation for $n=5$ (and to a lesser extent for $n=6$ and 12) is not as good, owing to lower quality of the global-fit data. Fortunately, it is pos-

sible to make improvements based on the semi-empirical polarization theory discussed next.

V. THE POLARIZATION FORMULA AND A SEMIEMPIRICAL THEORY

In the traditional polarization formula,[1] $\Delta^{(nr)}$ in Eq. (18) is called the polarization shift,

$$\Delta_p = A(Z)P(n,L)[1+k(Z)q(n,L)] \ . \tag{23}$$

$A(Z)=(Z-1)^4\alpha_1$, where α_1 is the dipole polarizability of the core[3] and has the value $\frac{9}{32}a_0^3$ for He. In Eq. (23), $P=(Z-1)^{-2}\langle r^{-4}\rangle$ and $q=(Z-1)^{-2}\langle r^{-6}\rangle/\langle r^{-4}\rangle$ are for the present purpose conveniently tabulated by Edlén.[23] However, owing to the difference in the reduced mass, those P values should be multiplied by 0.999 884 for helium. In a standard Edlén plot, $(\Delta p/P)$ is the ordinate and q the abscissa, therefore Ak is the slope and A the intercept.

Litzén[24] has applied the above formula to older data in helium[8] ($Z=2$). He concluded that the $(3-6)D$ data formed a straight line with slope -0.05 and intercept 0.277, while the $5G$ and the $(4-8)F$ shifts lay on a different line with slope $+1.8$ and intercept 0.240. Since the two lines had opposite signs for the slope and neither had the correct value for the intercept of $A=0.281\,25$, he justifiably questioned the usefulness of the polarization formula.

It is instructive to examine the implications of Drachman's theory for the polarization formula. In Eq. (23), the first term is practically the same as V_4 given by Eq. (20), except for the negligible correction factor of 1.000 006, imperceptibly changing the dipole polarizability α_1 from 0.281 250 to $0.281\,252a_0^3$. The next term in Eq. (23) is V_6, provided that $k(Z)=(\alpha_2-6\beta_1)/\alpha_1$, where[3] $\beta_1=\frac{43}{512}$ and $\alpha_2=\frac{15}{64}$. Now Eq. (22) can be easily described in terms of an Edlén plot. For $L>3$, all levels lie in a straight line with slope $(\alpha_2-6\beta_1)=-0.2694$ and intercept $\alpha_1=0.281\,25$, as long as the uncertainty in Eq. (22b) is negligibly small.

In Fig. 1, the quantity $\Delta^{(nr)}/P$ is plotted against q as in a standard Edlén plot for all $L>3$ levels from Table IV. The points (circles) computed from Eqs. (14), (17), and (18) clearly fit the straight line very well, with the expected slope $(\alpha_2-6\beta_1)$ and intercept $A=\alpha_1$. Clearly the error term and effects left out of Eq. (22b) are undiscernible, and the present procedure of fixing energies to an absolute scale is validated. A measure of the sensitivity of this plot is shown by accepting the $7\,^1F_3-{}^1I_6$ three-photon transition.[13] Then, the $7I$ level would be given by Drachman's theory, so the $7G$ and the $7H$ levels could be determined from the $7F$ by one- and two-photon measurements.[7,13] These results for $7H$ and $7G$ shown as triangles in Fig. 1 are seen to stray far off the line. The inconsistency of this difficult three-photon measurement with other results has been noted and thoroughly discussed by others.[3,14]

For $L=3$, Drachman's theory as given by Eq. (22a) predicts an Edlén plot whose slope has an uncertainty equal to its own value of -0.135 and whose intercept has the value of α_1, but with very large error bars. These undemanding requirements are well met by the present data in Fig. 2. They fall on a straight line as indicated except

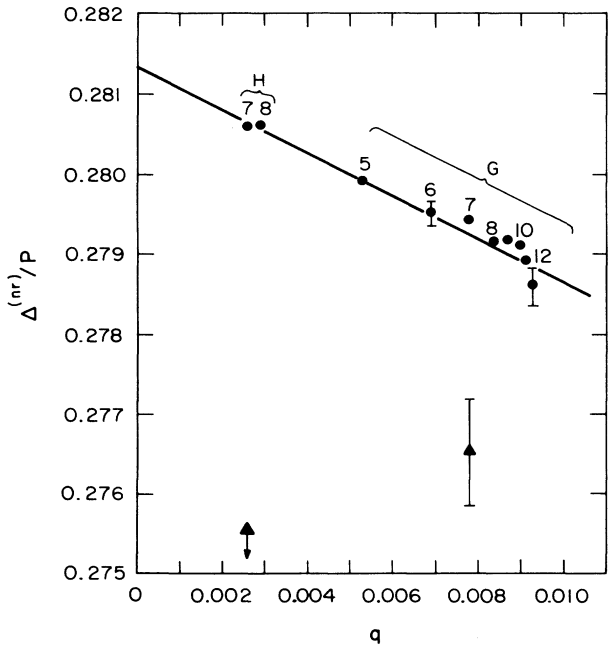

FIG. 1. Edlén plot for $L=4$: ●, present data, ▲ from Cok and Lundeen's $7I$-$6F$ measurements (↓ indicates off scale).

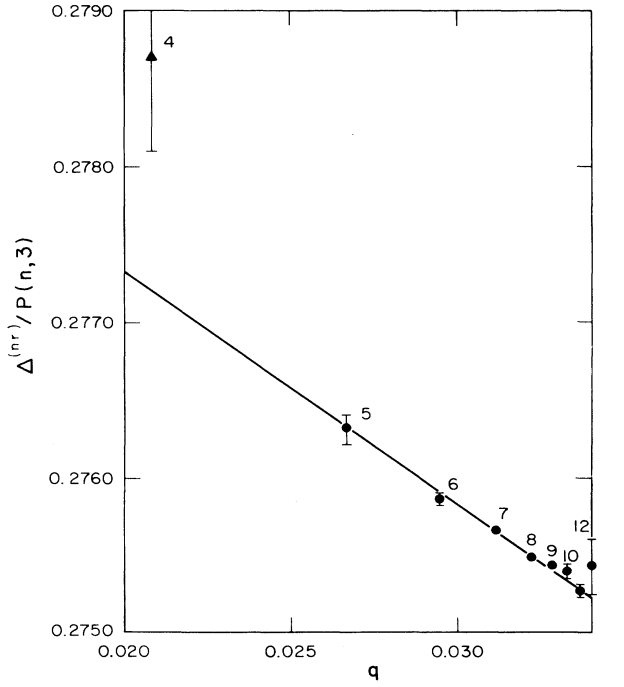

FIG. 2. Edlén plot for F states derived from Table IV. The $4F$ value is unreliable (see text), and is replaced by a point on the straight line in the improved semi-empirical term values (Table V).

for the unreliable point for $n=4$. The line yields a slope of -0.150 ($k=-0.535$) and $A=0.28036$ which differs from α_1 by 0.3%. It is recalled that Litzén's corresponding values for F levels are $+1.8$ and 0.240. These discrepancies are easily traced to his data[24] which deviate from the present by as much as 0.05 cm^{-1}. Both sets of energies will be compared with diode laser measurements in Sec. VI.

Next the Edlén plot for $L=2$ levels is shown in Fig. 3. Once more, the points form a straight line except for the $n=4$ one which is suspect (triangle). It should be replaced by the underlying circle which is derived from a semi-empirical theory to be discussed later. The slope and intercept are -0.04163 ($k=-0.1513$) and 0.27519, respectively, which are not very different from Litzén's values.[24]

The above straight-line behavior implies that effects left out of Eq. (22) scale as $q(n,L)$. As discussed by Drachman,[3] they are primarily $\Delta_{\rm pen}^{(0)}$ due to penetration of the optical electron into the core, $\Delta_{\rm pen}^{(1)}$ which accounts for the short-range correction to the asymptotic form of the dipole polarization potential, and $\Delta^{(2)}$ the second-order dipole polarization shift. The first and the last always lower the energy ($\Delta_{\rm pen}^{(0)},\Delta^{(2)}>0$), while the second raises the energy ($\Delta_{\rm pen}^{(1)}<0$).

Calculations show that all three effects decrease rapidly as L increases. Indeed for $L=4$ they are all negligibly small as implied by Fig. 1. For example, Drachman found that for the $8G$ level, $\Delta_{\rm pen}^{(0)}=1.4\times10^{-6}$, $\Delta_{\rm pen}^{(1)}=-2.4\times10^{-6}$, and $\Delta^{(2)}=1.2\times10^{-5}$ cm^{-1}. Actually the definition of $\Delta_{\rm pen}^{(1)}$ is not unique since there is not a "proper" way to cut off the dipole polarization potential. I have chosen the Bethe-Reeh[25] method of calculating the dipole polarization energy rather than the Callaway-Temkin cutoff employed by Drachman.[3] My value for $\Delta_{\rm pen}^{(1)}$ is -8.8×10^{-7} cm^{-1}

For the F levels, these effects are of the order of 10^{-3} cm^{-1} for the lower-n members and certainly not negligible. Drachman has reported $\Delta_{\rm pen}^{(0)}$ values for $n=7$ and 8, and the values for $n=4$ and 5 may be obtained from Heisenberg's two special-case formulas[14] for $n=L+1$ and $n=L+2$. In Fig. 4, where $\Delta_{\rm pen}^{(0)}/P(n,3)$ is plotted against $q(n,3)$, these four points (circles) fall on a straight line, as was first observed in Co IX by Vogel.[26] For $\Delta^{(2)}$, Drachman[4] has calculated all values with n ranging from 4 to 11 and I have computed $\Delta_{\rm pen}^{(1)}$ for the same n values. Similar to $\Delta_{\rm pen}^{(0)}$, these energy shifts are plotted in Fig. 4 in the same manner, with the former as triangles and the latter as squares. It is evident that both $\Delta^{(2)}$ and $\Delta_{\rm pen}^{(1)}$ form straight lines too. Not shown are the facts that $\Delta_{\rm pen}^{(1)}$ for $L=2$, $\Delta^{(2)}$ for $L=4$, 5, and 6 all form individual straight lines when divided by $P(n,L)$ and plotted against $q(n,L)$ for the same L. It seems reasonable to infer that all significant effects not accounted for in Eq. (22) scale with $q(n,L)$ for $L\geq2$. Since all three lines in Fig. 4 do not extrapolate to the origin, both the slope and the intercept in an Edlén plot will be modified by these shifts as in Figs. 2 and 3. That penetration effects scale with q for each L has been noted previously[2,26] but the observation for the second-order polarization shift appears to be new.

Since these shifts cannot all be calculated unambiguously (except through a full-scale variational computation, as by Kono and Hattori[6]), I favor the semi-empirical approach advocated by Curtis.[2] Like his semi-classical theory, three separate plots must be made for D, F, and G

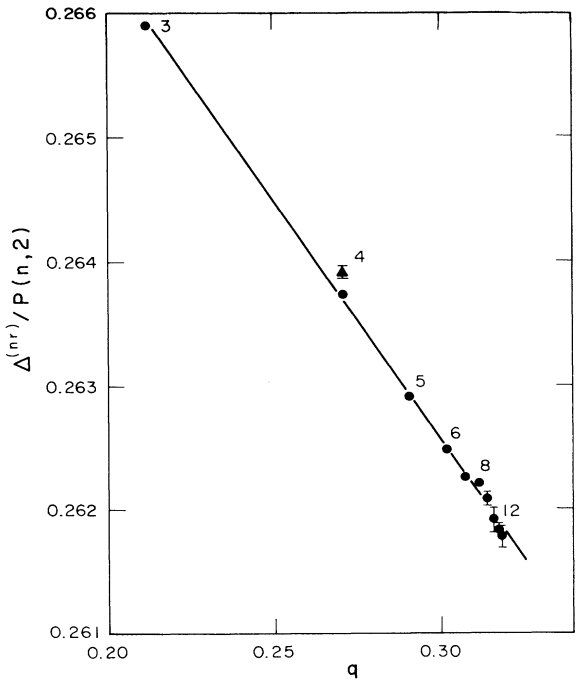

FIG. 3. Edlén plot for D states derived from Table IV. For $n=4$, the triangle is from Table IV and the circle from Table V. The $n=3$ value is derived from Martin (Ref. 9).

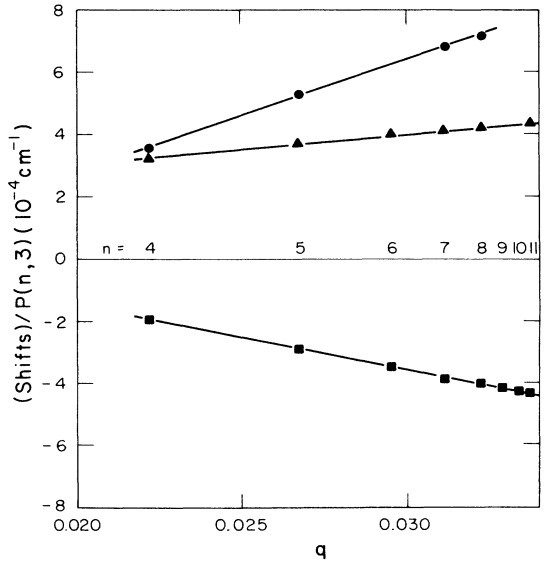

FIG. 4. Corrections to Drachman's results for F states in an Edlén plot. ●, penetration $\Delta_{\rm pen}^{(0)}$. ▲, second-order dipole polarization $\Delta^{(2)}$. ×, short-range dipole "cutoff" $\Delta_{\rm pen}^{(1)}$.

and all higher-L levels. Carrying this approach one step further, I note that the exchange energies in Table III do not scale exactly as n^{-3}. However, when $n^3X(n,L)$ is plotted against $q(n,L)$ the data form a straight line again. Therefore the Edlén plot can be used for the exchange as well as for the polarization energy.

The results for D levels are displayed in Fig. 5. On this scale, differences among the columns in Table III are not apparent. Upon closer scrutiny a small nonlinearity is evident, and the point for $n=3$ shows a significant departure from the straight line. I attribute these effects to the small but non-negligible penetration of D states which is most evident for the lowest level ($n=3$).

Figure 6 shows the same results for F levels. Here X values from Eq. (15) are shown as triangles and from Eq. (16) as inverted triangles (except when they coincide with the circles). Unfortunately, the difference in the two sets is rather large, and in the case of $n=4$, X evaluated from Eq. (16) even becomes complex. As discussed earlier in Sec. III, the discrepancy is a reflection of the progressively lower quality in the low-n global-fit data where reliance has to be placed on nonlinear extrapolations. Actually, improvements can be made by a judicious choice of experiment and theory. For $n=6$–11, the $^1F_3$-$^3F_3$ interval is already accurately measured by connection to the $^1D_2$. Reliable theoretical values may be taken from Table II for the $^3F_2$-$^3F_4$ interval. Then Eq. (16) yields X values shown as circles in Fig. 6. Working backwards it is now also possible to redetermine the term values and the new X from Eq. (15). These new X's from the two equations now agree to better than 1%. The new values usually lie between the two old ones, and, more importantly, they now form a well-determined straight line. Although the $n=5$ $^1F_3$-$^3F_3$ interval in the global-fit data has been determined through extrapolation, when combined with the theoretical $^3F_2$-$^3F_4$ interval, a consistent X value is obtained. Further, the new X (circle) lies on the same line in Fig. 6. Therefore, the $5\,^1F$—^3F interval is accepted as accurate. However, that is not the case for $n=4$. Here straight-line extrapolation in Fig. 6 yields 0.083(2) cm^{-1} for n^3X. Table III shows that this value for X differs from the old one by more than a factor of 2. Finally, the value for the direct energy D is calculated from the straight-line extrapolation in Fig. 2 of $\Delta^{(nr)}/P(4,3) = 0.277\,23(4)a_0^3$. From these values, new or improved term values are calculated and listed in Table V. Since no significant improvement is found for the higher values of n, new term values for $n \geq 7$ are not given.

For the D levels, the global-fit data are based on experimental $^1D_2$-$^3D_2$ intervals only for $n \geq 7$, which are then extrapolated to lower n. For $n=6$, the measurements of Beyer and Kollath[27] place the ^3D_J term values at 0.000 18(31) cm^{-1} higher than those in Table IV and are judged to be less accurate. On the other hand, the $5\,^1D$—$5\,^3D_{av}$ measurement[28] of 1.136 32(6) cm^{-1} is a substantial improvement over the global-fit extrapolation. Defining the average ^3D level as the $(2J+1)$-weighted average of the triplet levels in Eq. (12), the difference $(^3D_{av} - ^3D_2)$ is found to be $[h + 3L(L+1)h^2/X]$, which has a value of 0.001 65 cm^{-1} using values of h and X from Tables II and III. Combining with the previously determined $5\,^1D_2$ term value, the improved $5\,^3D_2$ value is 4392.517 05(8) cm^{-1}. The $5\,^3D_1$ and $^3D_3$ levels are then found relative to this new $^3D_2$ level from the accurate

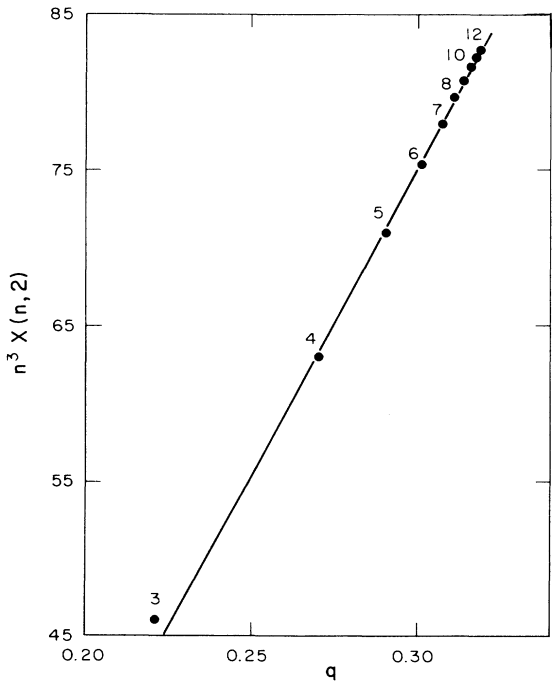

FIG. 5. Exchange energy in cm^{-1} for D states in an Edlén-like plot.

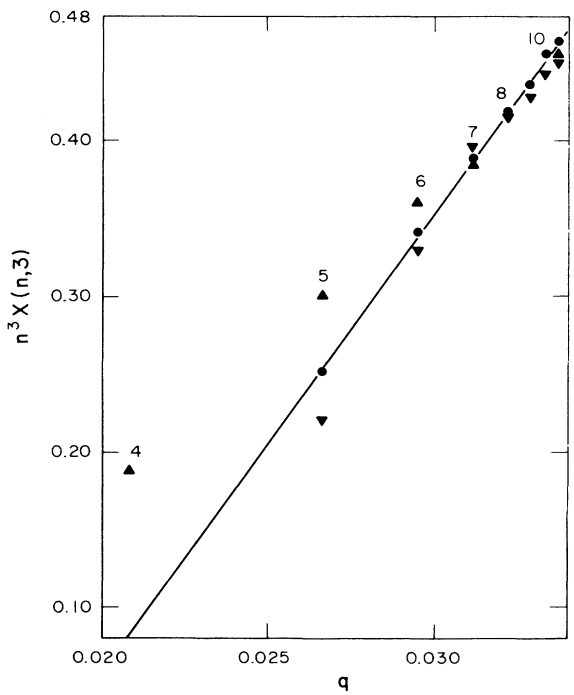

FIG. 6. Exchange energy in cm^{-1} for F states in an Edlén-like plot.

TABLE V. Improved term values (in cm^{-1}).

n	^{2S+1}L	J	
3	D		Martin[a]
4	^1F	3	6858.771 90(10)
	^3F	2	6858.775 42(10)
		3	6858.794 80(10)
		4	6858.784 05(10)
4	^1D	2	6864.212 45(41)
	^3D	1	6866.168 27(13)
		2	6866.186 78(13)
		3	6866.187 99(13)
5	G		Table IV
5	^1F	3	4389.538 21(10)
	^3F	2	4389.543 33(11)
		3	4389.550 66(11)
		4	4389.547 75(11)
5	^1D	2	4392.379 04(6)
	^3D	1	4393.507 53(8)
		2	4393.517 01(8)
		3	4393.517 65(8)
6	G		Table IV
6	^1F	3	3048.237 16(4)
	^3F	2	3048.240 55(4)
		3	3048.244 72(4)
		4	3048.243 11(4)
6	D		Table IV

[a]Reference 9 combined with E_I from Table IX.

magnetic dipole transitions and listed in Table V. For the $4D$ state, the global-fit data give the ^1D term value to a precision of 41×10^{-5} cm^{-1} by averaging the transitions to the $4\,^3F_3$ and the $4\,^1F_3$. For the $4\,^3D$ states, substantially better term values may be obtained from the difference of the $2\,^3S_1-4\,^3D_1$ and $2\,^3S_1-5\,^3D_1$ measurements.[29] Thus the $4\,^3D_1$ level is calculated from the $5\,^3D_1$ level in Table V by adding 2472.660 70(10) cm^{-1}. As before the $4\,^3D_2$ and $4\,^3D_3$ are then found from the magnetic dipole transitions. These new sublevels are all given in Table V. They are found to give more consistent X values than those in Table IV. These improved X values for $L=2$ and 3 are given in the last column of Table III. Shown in Fig. 3, the improved energy shifts $\Delta^{(nr)}$ for $n=5$ and 6 are essentially the same as the old values for Table IV, but the new value for $n=4$ now falls on the straight line. As indicated in Table V, the $3D$ term values have to be derived from Martin's energies[9] and the ionization potential (Sec. VII).

VI. MULTIPLET LINE INTENSITIES AND A DIODE LASER MEASUREMENT

The above energy-level scheme will now be tested against laser measurements. For direct comparison with experiment, it is useful to have the multiplet line intensities. In a rigorous L-S coupling scheme, the triplet values have been given by Bethe and Salpeter.[17] A more general formula for arbitrary S is[18]

$$I=(2J+1)(2J'+1)\begin{Bmatrix}1 & J & J'\\ S & L' & L\end{Bmatrix}^2 . \tag{24}$$

To account for singlet-triplet mixing when $J=L$, it is advantageous to introduce a mixing angle θ_L such that

$$\tan(2\theta_L)=(Z+1)h\sqrt{L(L+1)}/[X+(Z-1)h/2] . \tag{25}$$

From Tables II and III, θ_L is easily calculated. It varies slowly with n, recalling the n^{-3} dependence of h and X. However, it changes rapidly from 0.5° to 30° to 44° for $L=2$, 3, and 4, respectively. Note that 0° corresponds to no mixing (rigorous L-S coupling) and 45° to complete mixing. Then in terms of L-S wave functions ϕ_{LS}, the actual wave functions in the coupled representation are given by

$$\psi_{L\,0L}=\phi_{L\,0}\cos\theta_L+\phi_{L\,1}\sin\theta_L ,$$

and

$$\psi_{L\,1L}=-\phi_{L\,0}\sin\theta_L+\phi_{L\,1}\cos\theta_L . \tag{26}$$

Now the relative line intensities may be evaluated in the usual electric dipole approximation from Eq. (26). For the transition $^{2S+1}L_J$-$^{2S'+1}(L+1)_{J'}$; they are displayed in Table VI. For high L (≥4) transitions, θ_L is nearly 45°, so the diagonal transitions in Table VI are of order unity while the nondiagonal ones are smaller by at least $(2L+2)^{-2}$ or 2 orders of magnitude. Therefore one can usually observe only the four diagonal transitions as noted by Lundeen.[13,16]

In a recent diode laser absorption experiment,[10] the $5D$-$6F$ singlet and triplet transitions have been measured to an accuracy of 0.001 cm^{-1}. Nevertheless, the Doppler width of about 0.008 cm^{-1} precluded the resolution of the triplet fine structure. As observed by Nagai *et al.*[10] their transition frequencies differed considerably from those obtained through Martin's compilations.[8,9] Also shown in Table VII are the many-body calculations[12] which, although in reasonable agreement with Martin, are not in

TABLE VI. Multiplet intensities for $^{2S+1}L_J$-$^{2S'+1}(L+1)_{J'}$. $\lambda=(L+1)^{-1}$; $\gamma=\sqrt{L(L+2)}/(L+1)$; C,S=cos, sin with the first argument always θ_L and the second θ_{L+1}.

S,J \ $S'J'$	$0,L+1$	$1,L+1$	$1,L$	$1,L+2$
$0,L$	$(CC+SS\gamma)^2$	$(-CS+SC\gamma)^2$	$(\lambda\sin\theta_L)^2$	0
$1,L$	$(-SC+CS\gamma)^2$	$(SS+CC\gamma)^2$	$(\lambda\cos\theta_L)^2$	0
$1,L-1$	0	0	$(2L-1)/(2L+1)$	0
$1,L+1$	$(\lambda\sin\theta_{L+1})^2$	$(\lambda\cos\theta_{L+1})^2$	$\lambda^2/(2L+1)/(2L+3)$	$(2L+5)/(2L+3)$

TABLE VII. Transitions providing a critical test (in cm^{-1}; E=experiment, T=theory).

Methods	$5\,^1D-6\,^1F$	$5\,^3D-6\,^3F$
Diode laser (E)[a]	1344.1404(10)	1345.2712(10)
Martin (E)[b]	1344.1089(90)	1345.2470(100)
Many-body (T)[c]	1344.0931	1345.2123
Variational (T)[d]	1344.1440(90)	1345.2798(90)
Present	1344.1399(2)	1345.2721(3)

[a]Reference 10.
[b]References 8 and 9.
[c]Reference 12.
[d]Reference 6 for D and Ref. 11 for F levels.

accord with the laser data. In contrast, variational calculations[6] are in excellent accord with these high-precision data.

For comparison with the present work, multiplet line intensities are calculated from Table VI, where the mixing angles for the $5D$ and $6F$ states are calculated from Tables II and III to be 0.58° and 31.31°, respectively. Taking the improved term values from Table V, the fine-structure transition for frequencies and intensities are given in Table VIII. It is evident that the frequencies separate cleanly into a "singlet" at 1344.14 and a "triplet" at 1345.27 cm^{-1} when viewed with a width of 0.01 cm^{-1}. In the actual measurement, the line position was determined from the second derivative of the intensity.[10] Effectively this introduced a frequency cutoff factor of half width 0.004 cm^{-1} into the signal profile (assuming room temperature and that the diode laser width was less than 0.002 cm^{-1}). Thus, the measured line positions corresponded approximately to the weighted mean of certain multiplet frequencies provided they fell within 0.008 cm^{-1} of each other. Applying this criterion in Table VIII results in a mean single value of 1344.1399(2) and a mean triplet value of 1345.2721(3) cm^{-1}. As can be seen in Table VII, these values are in excellent agreement with the laser measurements. Had the global-fit energies been used, the singlet result would be unchanged, but the triplet result would be 0.0006 cm^{-1} closer to experiment.

TABLE VIII. $5D$-$6F$ fine-structure frequencies and intensities. The measured "singlet" corresponds to the weighted mean of the first three frequencies, while the "triplet" corresponds to the next four.

$5D$		$6F$			
S	J	S'	J'	σ (cm^{-1})	Relative intensity
0	2	1	3	1344.1343	0.26
0	2	1	2	1344.1385	0.00
0	2	0	3	1344.1419	0.74
1	1	1	2	1345.2669	0.6
1	2	1	3	1345.2722	0.66
1	3	1	3	1345.2728	0.08
1	3	1	4	1345.2744	1.29
1	2	1	2	1345.2764	0.11
1	3	1	2	1345.2770	0.00
1	2	0	3	1345.2798	0.23
1	3	0	3	1345.2804	0.03

VII. THE IONIZATION ENERGY

Another test of the term levels is to see if they consistently lead to a correct ionization energy. Previously, Martin[9] has obtained a value of 198 310.7745(40) cm^{-1}, with the understanding that the experimental value for the $2\,^1P$ level has been arbitrarily extended to four decimal places (from one) to fix the excited-term system. From large-scale variational calculations, Kono and Hattori[6] first obtained a value of 198 310.7730(10) and very recently[30] 198 310.7725(5) cm^{-1}. Substituting the present semiempirical term values for their variationally computed ones, I obtain the values listed in Table IX as described below.

The ionization energies from D states are obtained simply by adding the term values in Table IX to the energy levels of Martin.[9] Quoted errors represent the square root of the sum of squared errors. For the F states, E_I cannot be reliably derived from Martin's energy level (e.g., his $5\,^1F$ value fell short by 0.03 cm^{-1}). Fortunately, the $6F$ energy levels can be determined by adding the measured diode laser frequencies to Martin's $5D$ levels. However, the singlet and the triplet energies thus found are weighted averages and similarly weighted term values from Table V must be added to give the ionization energies. The errors here are due almost solely to the laser measurements. The ionization energies in Table IX are averaged by the usual procedure[9] to yield an ionization limit of 198 310.7722(5) cm^{-1}. This value is totally consistent with and more accurate than those of Martin[9] and of Kono and Hattori[6] given earlier, and subject to the same assumption on the $1\,^1S-2\,^1P$ measurement.

TABLE IX. The ionization energy. Term values from Table V are added to their experimental energies from Martin (Ref. 9) to give E_I. The averaged term values are discussed in the text.

Term	E_I (cm^{-1})
$4\,^1D_2$	198 310.7714(20)
$5\,^1D_2$	198 310.7722(5)
$6\,^3D_3$	198 310.7727(9)
$6\,^3F_{av}$	198 310.7713(11)
$6\,^1F_{av}$	198 310.7726(11)
Limit	198 310.7722(5)

VIII. SUMMARY AND CONCLUSIONS

Experimental data on the fine structure of Rydberg levels in helium have been coalesced into a unified set of term values. They are accurately described by semi-empirical formulas collected below conveniently for applications. Each fine-structure level is given by

$$E(n,L,S,J)=E_I-R/n^2-\Delta_{nL}^{(r)} -F(n,L)-W(n,L,S,J)\ . \tag{27}$$

In Eq. (27), E_I and R can be found in Table X, and $\Delta_{nL}^{(r)}$ has been given by Eq. (19). The spin-free energy is semi-empirically represented by

$$F(n,L)=P(n,L)[A(L)+B(L)q(n,L)]\ . \tag{28}$$

and the fine-structure splitting is, according to Eq. (12),

$$W(n,L,1,L-1)=X-(L+1)(2L+1)h/(2L-1)\ ,$$
$$W(n,L,1,L+1)=X+L(2L+1)h/(2L+3)\ , \tag{29}$$
$$W(n,L,1,L)=h/2+[(X+h/2)^2+9L(L+1)h^2]^{1/2}\ ,$$

and

$$W(n,L,0,L)=h/2-[(X+h/2)^2+9L(L+1)h^2]^{1/2}\ .$$

For easy reference, Eqs. (19) and (6) are repeated here,

$$\Delta_{nL}^{(r)}=\alpha^2R[n/(L+\tfrac{1}{2})-\tfrac{3}{4}]/n^4\ ,$$
$$h(n,L)=\alpha^2R/[n^3(2L+1)L(L+1)]\ ,$$

and X has been empirically found to be

$$X(n,L)=[C(L)+D(L)q(n,L)]/n^3\ . \tag{30}$$

The empirical constants A, B, C, and D are displayed in Table X for all $L\geq 2$. Finally, the scaling factors in the polarization formulas[1,23] are

$$P(n,L)=\frac{R[3n^2-L(L+1)]}{[2n^5(L-\frac{1}{2})L(L+\frac{1}{2})(L+1)(L+\frac{3}{2})]}\ ,$$

and

$$q(n,L)=R\{35n^4-5n^2[6L(L+1)-5] +3(L-1)L(L+1)(L+2)\} \times[8n^7(L-\tfrac{3}{2})(L-1)(L-\tfrac{1}{2})L(L+\tfrac{1}{2})(L+1) \times(L+\tfrac{3}{2})(L+2)(L+\tfrac{5}{2})P(n,L)]^{-1}\ . \tag{31}$$

TABLE X. Parameters for semi-empirical theory. $E_I=198\,310.7722\ \text{cm}^{-1}$. $R=109\,722.2752\ \text{cm}^{-1}$.

L	A	B	C	D
2	0.275 19	−0.041 63	−45.2	401
3	0.280 36	−0.1500	−0.55	30
4	0.281 25	−0.2695	0	0

The semi-empirical theory given above should fit helium energy levels accurate to better than 0.001 cm^{-1}.

Although the present results as summarized in Eqs. (27)—(31) are not new term by term, they embody all known effects accurate to 10^{-5} cm^{-1} and are compatible with experiments. Further, these effects are grouped in such a manner as to facilitate generalization to other atoms. For example, the Rydberg constant for an N-electron system is evidently $R=m[M+(N-1)m]/(M+Nm)$. The near cancellation of mass polarization, relativistic correction of the core polarizability, and the retarded potential in He I is fortuitous. Nevertheless, there is no evidence that inclusion of the retarded potential worsens the agreement of theory with experiment.[3,14] (As pointed out in Refs. 22, the erroneous retarded potential term used in Refs. 3 and 14 overestimates by about an order of magnitude.) In view of the difficulty of calculating these effects in a larger atom, it is not unreasonable to delete all three. The linearity of the spin-free energy has already been found[2] in Si III. The fine-structure theory in Sec. II is formulated for the general case where the core can have any arbitrary spin.

The general implications of this work for the polarization formula seem clear. The usefulness of Edlén plot is diminished in one respect, but enhanced in another. Since separate plots must now be made for each value of L until L is sufficiently large ($L=4$ for helium), the procedure requires a lot more data before it is beneficial. On the other hand, one can now expect straight-line behavior not only for the direct but also for the exchange energy. In view of these considerations, it will be very interesting to reexamine a similar system such as Mg I, where the core polarizability is 100 times larger.[31] Another interesting application of the present work is to systems whose core has a spin other than $\frac{1}{2}$. High-L emission lines in O I have been recently observed and will be reported elsewhere.

ACKNOWLEDGMENTS

I thank Wit Bucko for carrying out some computations. I am grateful to W. C. Martin for useful correspondence and stimulating conversations. Helpful comments from S. R. Lundeen, G. Herzberg, R. J. Drachman, and L. J. Curtis are appreciated.

APPENDIX: EVALUATION OF THE TERM VALUES

For the $n=5$ manifold, Δ_{5G} is taken from Drachman's theory[3,32] to be 0.15598(3) cm^{-1}. The $5G$ term value is then calculated from Eqs. (17)—(19) to be 4389.05036 cm^{-1}. From Eq. (12), the shift of the $5\,^1G$ sublevel is $-0.003\,35$ cm^{-1}. Therefore, the term value of $^1G_4$ is given in Table IV as 4389.047 01(3) cm^{-1}. Other sublevels are now located by the following transitions given by Farley *et al.*,[7] with the error in 10^{-5} cm^{-1} in parenthesis: $^1D_2$-$^1G_4$ (8), $^1D_2$-$^3G_4$ (14), $^1D_2$-$^1F_3$ (6), $^1D_2$-$^3F_3$ (6), $^3D_2$-$^1D_2$ (33), $^3D_3$-$^1F_3$ (32), $^3D_2$-$^3D_1$ (1), $^3D_3$-$^3G_3$ (34), $^3D_3$-$^1F_3$ (32), $^3D_2$-$^3D_1$ (1), $^3D_3$-$^3G_3$ (34), $^3D_3$-$^3G_5$ (36), $^3D_3$-$^3F_2$ (36), and $^3D_3$-$^3F_4$ (37), and are listed in Table IV. In the $n=5$

manifold, no measurements are available for transitions between sublevels of different L. So those transitions used have been derived by extrapolation from higher values of n, and are judged to be much less reliable than the stated errors.

1. The $n=6$ manifold

Since no experimental data are available for the $6H$ states, I begin with the $6G$. According to Drachman, $\Delta_{6G}=0.100\,15(4)$ cm^{-1}. From Eqs. (17) and (18), we find that $t_{6G}=3047.943\,78(4)$ cm^{-1}, where the number in parenthesis is the error in the last digit. Now the only accurately measured transition from the $6G$ level is the $6\,^1F_3$–$6\,^1G_4$ (0.295 34 cm^{-1}). I therefore calculate the term value of the $6\,^1G_4$ level from Eq. (12) and obtain 3047.941 82(4) cm^{-1}. Hence, the position of the $6\,^1F_3$ is 3048.237 16(4). Similarly from MacAdam's $6\,^1D_2$–$6\,^1F_3$ transition[7] (1.661 26 cm^{-1}), the $6\,^1D_2$ term value is determined to be 3049.898 42(4) cm^{-1}. Other sublevels are obtained from the global fit data of Farley *et al.*[7] (error in 10^{-5} cm^{-1}) $^1D_2$-$^3G_2$ (2), $^3D_2$-$^1D_2$ (5), $^1D_2$-F_3 (1), $^3D_2$-$^3D_1$ (1), $^3D_3$-$^3D_2$ (1), $^3D_3$-$^3F_4$ (7), $^3D_3$-$^3F_2$ (7), $^3D_3$-$^3G_3$ (6), and $^3D_3$-$^3G_5$ (6). Other given transitions within the $n=6$ manifold are used to check for internal consistency. From each L complex, the spin-free term value is found from Eq. (14) to be 3047.943 78(4), 3048.240 77(4), and 3050.247 34(5) cm^{-1} for $L=4$, 3, and 2.

As discussed in Sec. V, the $7\,^1F_3$–$^1I_6$ measurement[13] is considered unreliable. So I begin with the H level, where Δ_{7H} has been calculated[3] to be 0.022 21(0) cm^{-1}. Following the same procedure when $n=5$, we find $t_{7H}=2239.253\,57$ cm^{-1}, and the shift of the $7\,^1H_5$ sublevel to be $-0.000\,82$ cm^{-1}. Hence, the term value of 2239.252 75 cm^{-1} for the $7\,^1H_5$ substrate is entered into Table IV. The other sublevels are determined from the two-photon transition measurements[13] $^1F_3$-$^1H_5$ (1), $^3F_2$-$^3H_4$ (1), $^3F_4$-$^3H_6$ (0), and $^3F_3$-$^3H_5$ (1) and the global-fit data[7] $^1D_2$-$^1F_3$ (0), $^1D_2$-$^3F_3$ (0), $^1D_2$-$^1G_4$ (0), $^1D_2$-$^1G_4$ (0), $^1D_2$-$^3G_4$ (0), $^3D_3$-$^1F_3$ (1), $^3D_3$-$^3D_2$ (0), $^3D_3$-$^3D_1$ (0), $^3D_3$-$^3F_4$ (1), $^3D_2$-$^3F_2$ (1), $^3D_3$-$^3G_5$ (1), and $^3D_3$-$^3G_3$ (1). It is gratifying that the $7\,^3H$ sublevels thus found are in perfect agreement with our theory [Eq. (12)].

Similarly for the $n=8$ level, it is found that $\Delta_{8H}=0.015\,77(0)$ cm^{-1}, $t_{8H}=1714.427\,32(0)$ cm^{-1}, and the term value for $8\,^1H_5=1714.426\,76(0)$ cm^{-1}. The $^1F_3$-$^1H_5(1)$ transition is utilized to determine the $8\,^1F_3$ sublevel in Table IV. Except for the $8\,^3H$ sublevels which are calculated from Eq. (12), all other sublevels are obtained from the global-fit transitions $^3D_3$-$^1F_3$ (0), $^1D_2$-$^1F_3$ (0), $^3D_3$-$^3F_3$ (0), ^3D_e-$^3F_4$ (0), $^3D_2$-$^3F_2$ (0), $^3D_2$-$^3F_2$ (0), $^3D_1$-$^3F_2$ (0), $^3D_3$-$^3G_4$ (1), $^3D_3$-$^3G_5$ (1), $^3D_2$-$^1G_4$ (0), and $^3D_2$-$^3G_3$ (1).

Since the cases for $n=9$–12 are very similar, they are discussed together below. Starting with the G levels, $\Delta^{(nr)}$ for $n=9$ and 10 have been tabulated[3] as 0.033 37(2) and 0.024 74(2) cm^{-1}, respectively. The corresponding values for $n=11$ and 12 can be calculated from Drachman's Eq. (47) using well-known expectation values[33] of x^{-s} to be 0.018 81(1) and 0.014 63(1) cm^{-1}. The hydrogen term values for the $9G$, $10G$, $11G$, and $12G$ states are 1354.597 11, 1097.223 61, 906.796 34, and 761.960 78 cm^{-1}, respectively. From Eq. (12), the corresponding shifts of the ^1G sublevels are easily found to be $-0.419\,05$ cm$^{-1}/n^3$. Thus, the term values for the $9\,^1G$, $10\,^1G$, $11\,^1G$, and $12\,^1G$ are, respectively, 1354.629 91(2), 1097.247 93(2), 906.814 83(1), and 761.975 17(1) cm^{-1}. For each of the above values of n, the other sublevels are evaluated from these global-fit transitions: $^1D_2$-$^1G_4$ (0), $^1D_2$-$^3G_4$ (0), $^3D_2$-$^1G_4$ (0), $^3D_2$-$^3G_3$ (0), $^3D_3$-$^3G_4$ (0), $^3D_3$-$^3G_5$ (1), $^3D_1$-$^3G_3$ (1), $^3D_3$-$^3F_3$ (0), $^3D_3$-$^3F_4$ (1), $^3D_3$-$^1F_3$ (0), and $^3D_1$-$^3F_2$ (0).

In the case of $n=12$, no experimental data exist for any D-G transitions. The corresponding global-fit transitions used above have been obtained through extrapolation in n. Therefore, the absolute term values of $12F$ and $12G$ sublevels are less accurate than the stated uncertainties as was the case for $n=5$.

Finally, term values for higher values of L not found in Table IV can be calculated to an accuracy of 10^{-5} cm by the same procedure.

[1] B. Edlén, *Atomic Spectra*, Vol. 27 of *Handbuch der Physik* (Springer-Verlag, Berlin, 1964).

[2] L. J. Curtis, Comments At. Mol. Phys. **16**, 1 (1985).

[3] R. J. Drachman, Phys. Rev. A **26**, 1228 (1982).

[4] R. J. Drachman, Phys. Rev. A **31**, 1253 (1985).

[5] D. R. Cok and S. R. Lundeen, Phys. Rev. A **19**, 1830 (1979); **24**, 3283(E) (1981).

[6] A. Kono and S. Hattori, Phys. Rev. A **31**, 1199 (1985).

[7] J. W. Farley, K. B. MacAdam, and W. H. Wing, Phys. Rev. A **20**, 1754 (1979).

[8] W. C. Martin, J. Phys. Chem. Ref. Data **2**, 257 (1973).

[9] W. C. Martin, Phys. Rev. A **29**, 1883 (1984).

[10] K. Nagai, T. Tanaka, and E. Hirota, J. Phys. B **15**, 341 (1982).

[11] J. S. Sims, D. R. Marmer, and J. M. Reese, J. Phys. B **15**, 327 (1982).

[12] T. N. Chang and R. T. Poe, Phys. Rev. A **10**, 1981 (1974); **14**, 11 (1976).

[13] D. R. Cok and S. R. Lundeen, Phys. Rev. A **23**, 2488 (1981).

[14] L. J. Curtis and P. S. Ramanujam, Phys. Rev. A **25**, 3090 (1982).

[15] W. Heisenberg, Z. Phys. **39**, 499 (1926).

[16] S. L. Palfrey and S. R. Lundeen, Phys. Rev. Lett. **53**, 1141 (1984); S. L. Palfrey, Ph.D. Thesis, Harvard University, 1984 (unpublished).

[17] H. A. Bethe and E. E. Salpeter, *Quantum Mechanics of One- and Two-Electron Atoms* (Academia, New York, 1957).

[18] U. Fano and G. Racah, *Irreducible Tensional Sets* (Academic, New York, 1957).

[19] J. C. Slater, *Quantum Theory of Atomic Structure* McGraw-Hill, New York, 1960), Vols. I and II. The average energy of a configuration is $E_{av}=D-X/2$, where $X=\sum_k \binom{l_0\ l\ k}{0\ 0\ 0}^2 \times G^k(l_0,l)$. The squared quantity is the Wigner 3-j symbol, G is the Slater exchange integral, and l_0 is the orbital angular

momentum of the open-shell electron(s).
[20]R. J. Drachman, Phys. Rev. A **33**, 2780 (1986).
[21]A. I. Ferguson, Phys. Bull. **37**, 330 (1986).
[22]C. K. Au, Gr. Feinberg, and J. Sucher, Phys. Rev. Lett. **53**, 1145 (1984).
[23]B. Edlén, Phys. Scr. **17**, 564 (1978).
[24]U. Litzén, Phys. Scr. **2**, 103 (1970).
[25]H. Reeh, Z. Naturforsch. A **15**, 377 (1960).
[26]P. Vogel, Nucl. Instrum. Meth. **110**, 241 (1973).
[27]H. J. Beyer and K. J. Kollath, J. Phys. B **10**, L5 (1977).
[28]G. G. Tepahan, H. J. Beyer, and H. Kleinpoppen, J. Phys. B **18**, 1127 (1985).
[29]L. Hlousek, S. A. Lee, W. M. Fairbank, Jr., Phys. Rev. Lett. **50**, 328 (1983).
[30]A. Kono and S. Hattori, Phys. Rev. A **34**, 1727 (1986).
[31]E. S. Chang and R. W. Noyes, Astrophys. J. **275**, L11 (1983).
[32]Conversion factor is 1 MHz $=3.335\,64\times10^{-5}$ cm^{-1}. In accordance with Eq. (20), the mass polarization correction in Drachman's results should now be removed.
[33]K. Bockasten, Phys. Rev. A **9**, 1087 (1974).